

up to 1000°C (Thermoflex thermoanalyzer). A further rise in temperature leads to solid phase reactions, the end product of which is zirconosilicate of the NASICON type and Na, Si glass.

Our analysis leads us to the conclusion that the crystals of the lovozerite family in their structural features satisfy the requirements for potential superionic conductors, in which the conductivity may be due to transport of Na atoms and H atoms. To these features we must refer the presence of a three-dimensional network of conductivity channels and statistical filling of the crystallographically equivalent positions with Na atoms with distances Na-Na = 3.2 and 3.6 Å; the structural disorder of compounds of the lovozerite type is a sign of the structure itself and does not require complication of the composition on account of heterovalent substitution, as, for example, in the structure of  $\text{Na}_4\text{Zr}_2\text{Si}_3\text{O}_{12}$ . This system enables us to create wide isovalent substitutions in the series Zr-Hf-Sn-Ti, and the presence of a large number of H atoms makes the lovozerite crystal a possible proton conductor.

<sup>1</sup>H. Hong, *Mater. Res. Bull.* **11**, 173 (1976).

<sup>2</sup>H. Hong, *Fast Ion Transport Solids*, North Holland (1979), p. 431.

<sup>3</sup>R. D. Shannon, H.-Y. Chen, and T. Berzina, *Mater. Res. Bull.*, **12**, 969 (1977).

<sup>4</sup>G. D. Ilyushin, L. N. Dem'yanets, V. V. Ilyukhin, and N. V. Belov, *Dokl. Akad. Nauk SSSR* **271**, 1133 (1983) [*Sov. Phys. Dokl.* **28**, 603 (1983)].

<sup>5</sup>G. D. Ilyushin, A. A. Voronkov, V. V. Ilyukhin, et al., *Dokl. Akad. Nauk SSSR* **260**, 623 (1981) [*Sov. Phys. Dokl.* **26**, 808 (1981)].

<sup>6</sup>G. D. Ilyushin, A. A. Voronkov, N. N. Nevskii, et al., *Dokl. Akad. Nauk SSSR* **260**, 1118 (1981) [*Sov. Phys. Dokl.* **26**, 916 (1981)].

<sup>7</sup>V. V. Ilyukhin and N. V. Belov, *Dokl. Akad. Nauk SSSR* **131**, 176 (1960).

<sup>8</sup>V. V. Ilyukhin and N. V. Belov, *Kristallografiya* **5**, 200 (1960) [*Sov. Phys. Crystallogr.* **5**, 186 (1960)].

<sup>9</sup>A. A. Voronkov, N. G. Shumyatskaya, and Yu. A. Pyatenko, *Crystal Chemistry of Zirconium Minerals and Artificial Analogs* [in Russian], Nauka, Moscow (1978).

<sup>10</sup>Z. V. Pudovkina, N. M. Chernitsova, A. A. Voronkov, and Yu. A. Pyatenko, *Dokl. Akad. Nauk SSSR* **250**, 865 (1980) [*Sov. Phys. Dokl.* **25**, 69 (1980)].

<sup>11</sup>A. A. Voronkov, Z. V. Pudovkina, V. A. Blinov, et al., *Dokl. Akad. Nauk SSSR* **245**, 106 (1979) [*Sov. Phys. Dokl.* **24**, 132 (1979)].

<sup>12</sup>A. V. Khomyakov, *Dokl. Akad. Nauk SSSR* **237**, 199 (1977).

<sup>13</sup>N. V. Zayakina, I. V. Rozhdestvenskaya, I. Ya. Nekrasov, and T. P. Dadze, *Dokl. Akad. Nauk SSSR* **254**, 353 (1980) [*Sov. Phys. Dokl.* **25**, 669 (1980)].

<sup>14</sup>A. N. Safronov, N. N. Nevskii, V. V. Ilyukhin, and N. V. Belov, *Dokl. Akad. Nauk SSSR* **255**, 1114 (1980) [*Sov. Phys. Dokl.* **25**, 962 (1980)].

<sup>15</sup>Yu. L. Kapustin, Z. V. Pudovkina, and A. V. Bykova, *Zap. Vsesoyuz. Mineral. Obshch.* **103**, 551 (1974).

<sup>16</sup>O. D. Maurice, *Econ. Geol.* **44**, 4 (1949).

<sup>17</sup>I. Ya. Nekrasov and T. P. Dadze, *Essays in Physicochemical Petrology* [in Russian], Nauka, Moscow (1978), No. 8, p. 193.

Translated by S. G. Kirsch

## New data on the crystal structure of murmanite

R. K. Rastsvetaeva and V. I. Andrianov

*Institute of Crystallography, Academy of Sciences of the USSR*

(Submitted October 17, 1984)

*Kristallografiya* **31**, 82-87 (January-February 1986)

The structure of murmanite has been redetermined. The model is refined to  $R = 9.1\%$  in the anisotropic approximation. The principal difference between the new model and that previously suggested lies in the fact that the Na positions in the anionic part of the structure are occupied, but in the cation part are only statistically occupied. On the basis of the new structural data the mechanism of decomposition of lomonosovite and its conversion to murmanite is explained.

The structure of murmanite was first investigated in 1965.<sup>1</sup> The model found from projections (by the photographic method) contained a number of inaccuracies, and the proposed crystal-chemical formula of the mineral did not reflect the complexity of its chemical composition and even contradicted it. More complete and reliable data on the structure of murmanite are important for an understanding of the mechanism of the processes of weathering and leaching of minerals of the lomonosovite group.

For x-ray structural investigation we used a specimen of deep violet color with linear dimensions of  $0.3 \times 0.2 \times 0.1$  mm, suitable for exposure in a diffractometer. The photographic method revealed the characteristic elongation and diffuseness of the diffraction spots for the minerals of the lomonosovite group, and the width of the peaks measured on the diffractometer was  $2-6^\circ$ .

Since refinement of the structure on the basis of the coordinates from Ref. 1 was unsuccessful ( $R \approx 35\%$ ), the model was determined afresh in the framework of the unit cell in Ref. 1 with the parameters obtained from the auto-

diffractometer:  $a' = 5.349(5)$ ,  $b' = 7.080(7)$ ,  $c' = 11.733(12)$  Å,  $\alpha' = 93.39(2)$ ,  $\beta' = 98.80(2)$ ,  $\gamma' = 89.8(2)^\circ$ ,  $V' = 438.3$  Å<sup>3</sup>. The structure was determined by the direct method by the program system RENTGEN-75 (Ref. 2) with the aid of an experimental set of 708 independent  $I \geq 3\sigma_I$  (Syntex P2<sub>1</sub>, CuK $\alpha$  radiation). Refinement of the new model by the method of least squares in the isotropic approximation and the centrosymmetric variant with  $R = 15\%$  led to large fluctuations in the values of the thermal parameters (even to negative values). This indicated the need to take account of isomorphic impurities in the positions of both Ti and Na. The pseudoperiodicity in two directions, found in the rotation patterns, required doubling of the parameters  $a'$  and  $b'$ . The new values of the parameters were refined on an Enraf-Nonius automatic diffractometer:  $A = 10.535(5)$ ,  $B = 13.884(4)$ ,  $C = 11.688(14)$  Å,  $\alpha = 94.31(6)$ ,  $\beta = 98.62(8)$ ,  $\gamma = 89.81(3)^\circ$ ,  $V = 1685.4$  Å<sup>3</sup>,  $\rho(x\text{-ray}) = 3.00$  g/cm<sup>3</sup>.

Since the new set of experimental data (Enraf-Nonius, 18181  $\geq 2\sigma_I$ , Mo K $\alpha$  radiation,  $\sin\theta/\lambda \leq 0.59$ )

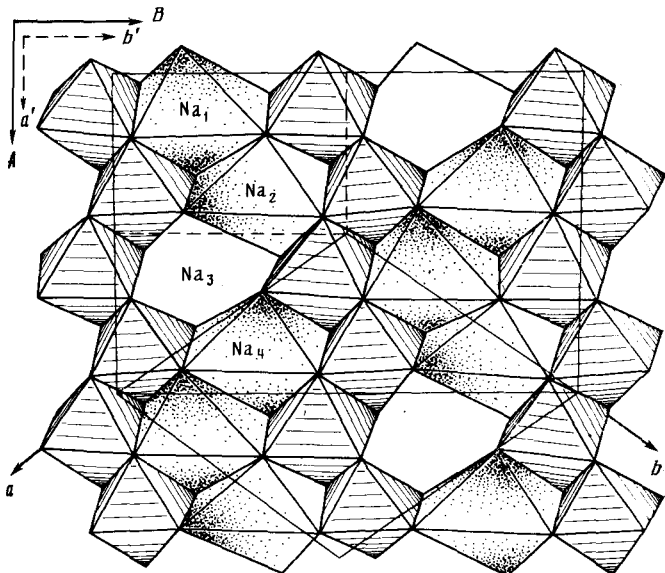


FIG. 1. Cation sheet projected on (001), showing three types of unit cell.

did not contain reflections with  $h + k \neq 2n$ , we changed to a primitive unit cell of smaller volume associated with the initial ratios  $a=(A-B)/2$ ,  $b=(A+B)/2$ ,  $c=C$ . Thus the parameters of the true unit cell of murmanite are as follows:  $a = 8.700(5)$ ,  $b = 8.728(4)$ ,  $c = 11.688(14)$  Å,  $\alpha = 94.31(6)$ ,  $\beta = 98.62(8)$ ,  $\gamma = 105.62(3)^\circ$ . The relationship between the three cells of murmanite is shown in Fig. 1; crystallochemical analysis is "tied" to the traditional unit cell for minerals of the lomonosovite group with axes A and B.

To avoid preconceptions further determination of the structure in the new cell was carried out in the acen-

tric group P1, adopted in Ref. 1 on the basis of the observed positive piezoeffect. To the initial model with  $R \approx 50\%$  was applied the phase correction procedure.<sup>3</sup> Six successive Fourier syntheses reduced the R factor to 30%, and the atoms were differentiated among the "titanium" and the "sodium" positions. In correspondence with the chemical composition, with allowance for the heights of the peaks on the electron density pattern and the requirements of local valence balance<sup>4</sup> to the Ti and Na positions we assigned atoms with mixed atomic curves. Refinement of the positional parameters of the final model with  $B_{tot} = 1$  led to  $R = 29\%$ . Attempts at further refinement gave no result. In connection with the sharply distinguished layer structure of the mineral, and also the strain and imperfection of the structure at this stage we refined the anisotropic coefficients of reduction of the set  $|F_{exp}|$  and  $|F_{theor}|$  (Ref. 5). This method was realized in the system of programs AREN-85<sup>1)</sup> and consists in the idea that into each value of  $F_{theor}$  we introduce a factor depending on six parameters, the values of which are refined by minimizing the functional

$$\Phi = \sum_H W_H (|F_{exp}| - K_H |F_{theor}|)^2,$$

where  $K_H = \frac{\sum_{ij} h_i a_i^* h_j a_j^* K_{ij}}{\sum_{ij} h_i a_i^* h_j a_j^*}$ ,  $h_1, h_2, h_3$  are the indices of the reflection,  $a_1^*, a_2^*, a_3^*$  are the parameters of the reciprocal lattice,  $K_{11}, K_{22}, K_{33}, K_{12}, K_{13}, K_{23}$  are the components of a symmetric tensor. Calculation of  $K_{11} = 1.188$ ,  $K_{22} = 1.195$ ,  $K_{33} = 0.451$ ,  $K_{12} = 0.472$ ,  $K_{13} = 0.220$ ,  $K_{23} = 0.030$  reduced the R index from 29 to 17.9%.

Further refinement in the isotropic approximation led to  $R = 13.5\%$ , and in the anisotropic to 9.1% (no cor-

TABLE I. Coordinates and Isotropic Thermal Parameters of Atoms (Å<sup>3</sup>)

Atom	x/a	y/b	z/c	B <sub>iso</sub>	Atom	x/a	y/b	z/c	B <sub>iso</sub>
Ti <sub>1</sub>	0.683	0.551	0.994	1.10	O <sub>11</sub>	0.973	0.100	0.088	2.02
Ti <sub>2</sub>	0.165	0.069	0.001	1.28	O <sub>12</sub>	0.992	0.899	0.924	2.30
Ti <sub>3</sub>	0.316	0.445	0.981	1.41	O <sub>13</sub>	0.491	0.612	0.074	2.13
Ti <sub>4</sub>	0.800	0.940	0.983	1.26	O <sub>14</sub>	0.305	0.491	0.265	0.85
Ti <sub>5</sub>	0.743	0.068	0.721	1.87	O <sub>15</sub>	0.522	0.377	0.290	1.57
Ti <sub>6</sub>	0.248	0.568	0.717	2.16	O <sub>16</sub>	0.686	0.876	0.275	2.29
Ti <sub>7</sub>	0.220	0.950	0.271	1.09	O <sub>17</sub>	0.231	0.193	0.289	0.49
Ti <sub>8</sub>	0.754	0.414	0.258	0.82	O <sub>18</sub>	0.508	0.395	0.907	2.07
Si <sub>1</sub>	0.142	0.187	0.742	1.64	O <sub>19</sub>	0.809	0.639	0.292	0.82
Si <sub>2</sub>	0.647	0.687	0.742	1.57	O <sub>20</sub>	0.159	0.243	0.893	1.59
Si <sub>3</sub>	0.143	0.537	0.222	1.53	O <sub>21</sub>	0.224	0.328	0.696	3.85
Si <sub>4</sub>	0.823	0.798	0.228	1.28	O <sub>22</sub>	0.993	0.416	0.247	1.53
Si <sub>5</sub>	0.613	0.009	0.215	0.96	O <sub>23</sub>	0.517	0.051	0.718	3.69
Si <sub>6</sub>	0.356	0.328	0.228	1.01	O <sub>24</sub>	0.014	0.540	0.725	4.30
Si <sub>7</sub>	0.344	0.965	0.766	1.89	O <sub>25</sub>	0.270	0.571	0.879	1.47
Si <sub>8</sub>	0.852	0.466	0.753	2.09	O <sub>26</sub>	0.692	0.852	0.697	4.28
Na <sub>1</sub>	0.905	0.303	0.988	0.10	O <sub>27</sub>	0.771	0.083	0.892	3.15
Na <sub>2</sub>	0.069	0.682	0.974	0.63	O <sub>28</sub>	0.211	0.026	0.714	3.86
Na <sub>3</sub>	0.381	0.805	0.004	1.97	O <sub>29</sub>	0.502	0.549	0.711	3.48
Na <sub>4</sub>	0.552	0.174	0.986	0.75	O <sub>30</sub>	0.947	0.141	0.712	2.16
Na <sub>5</sub>	0.983	0.177	0.272	1.37	O <sub>31</sub>	0.673	0.733	0.906	2.28
Na <sub>6</sub>	0.492	0.313	0.696	1.95	O <sub>32</sub>	0.342	0.995	0.915	2.43
Na <sub>7</sub>	0.985	0.809	0.705	2.39	O <sub>33</sub>	0.856	0.505	0.899	1.38
Na <sub>8</sub>	0.480	0.673	0.272	3.73	O <sub>34</sub>	0.315	0.769	0.722	1.94
O <sub>1</sub>	0.317	0.284	0.088	1.54	O <sub>35</sub>	0.816	0.634	0.726	2.72
O <sub>2</sub>	0.815	0.764	0.096	1.51	O <sub>36</sub>	0.817	0.274	0.721	3.06
O <sub>3</sub>	0.984	0.942	0.277	1.12	(H <sub>2</sub> O) <sub>1</sub>	0.249	0.982	0.459	3.16
O <sub>4</sub>	0.146	0.506	0.077	2.45	(H <sub>2</sub> O) <sub>2</sub>	0.775	0.446	0.460	2.59
O <sub>5</sub>	0.606	0.967	0.070	1.77	(H <sub>2</sub> O) <sub>3</sub>	0.998	0.230	0.453	3.73
O <sub>6</sub>	0.730	0.411	0.103	2.74	(H <sub>2</sub> O) <sub>4</sub>	0.473	0.767	0.451	1.95
O <sub>7</sub>	0.197	0.336	0.114	1.45	(H <sub>2</sub> O) <sub>5</sub>	0.988	0.762	0.521	4.12
O <sub>8</sub>	0.431	0.004	0.272	0.47	(H <sub>2</sub> O) <sub>6</sub>	0.500	0.255	0.505	2.80
O <sub>9</sub>	0.225	0.686	0.265	2.94	(H <sub>2</sub> O) <sub>7</sub>	0.691	0.054	0.534	3.34
O <sub>10</sub>	0.756	0.187	0.254	0.70	(H <sub>2</sub> O) <sub>8</sub>	0.208	0.547	0.536	2.97

Note. Standard deviations in coordinates: 0.001 for Si<sub>1-8</sub>, Ti<sub>1-8</sub>, and Na<sub>5-8</sub>; 0.002 for Na<sub>1-4</sub>; 0.002-0.005 for anions.

TABLE II. Characteristics of Polyhedra

Position	Coordination number	M-O distance		(O-O)	Possible isomorphous impurity
		range	mean		
Si <sub>1</sub>	4	1.44-1.77	1.63	2.65	Al  Fe <sup>3+</sup> , Mg  Al
Si <sub>2</sub>	4	1.46-1.90	1.65	2.66	
Si <sub>3</sub>	4	1.32-1.70	1.53	2.46	
Si <sub>4</sub>	4	1.54-1.67	1.61	2.61	
Si <sub>5</sub>	4	1.62-1.80	1.70	2.77	
Si <sub>6</sub>	4	1.45-1.66	1.60	2.59	
Si <sub>7</sub>	4	1.47-1.74	1.65	2.69	
Si <sub>8</sub>	4	1.47-1.71	1.61	2.57	
Ti <sub>1</sub>	6	1.85-2.19	2.02	2.84	Fe <sup>3+</sup>
Ti <sub>2</sub>	6	1.86-2.17	2.03	2.63	
Ti <sub>3</sub>	6	1.75-2.13	1.98	2.61	
Ti <sub>4</sub>	6	1.75-2.15	1.98	2.79	
Ti <sub>5</sub>	6	1.74-2.15	1.89	2.67	
Ti <sub>6</sub>	6	1.69-2.27	1.99	2.81	
Ti <sub>7</sub>	6	1.77-2.31	2.03	2.79	Nb
Ti <sub>8</sub>	6	1.78-2.34	2.02	2.85	
Na <sub>1</sub>	6	2.09-2.77	2.39	3.35	Mn, Fe <sup>2+</sup> , Zr, Nb Ca K
Na <sub>2</sub>	5	2.08-2.57	2.33	3.37	
Na <sub>3</sub>	5	2.08-2.63	2.28	3.33	
Na <sub>4</sub>	6	2.07-2.85	2.41	3.39	
Na <sub>5</sub>	6	1.98-2.19	2.09	2.95	
Na <sub>6</sub>	6	2.04-2.91	2.41	3.39	
Na <sub>7</sub>	8	1.88-3.00	2.51	3.20	
Na <sub>8</sub>	6	1.87-2.72	2.26	3.18	

Note. Error of determination of distances: 0.02-0.03 Å (Si-O); 0.03-0.04 Å (Ti-O) and 0.04-0.05 Å (O-O).

rection was made for absorption,  $\mu = 25 \text{ cm}^{-1}$ ). The thermal parameters of the atoms were assigned reasonable values.

The coordinates of the atoms and their thermal isotropic parameters are listed in Table I, and the main interatomic distances in Table II.

The mica-like structural motif of murmanite was described in Refs. 1 and 6. As also in the case of the allied minerals lomonosovite<sup>7</sup> and betalomonosovite,<sup>8</sup> it is based on infinite three-layer stacks parallel to (001) (Fig. 2). The individuality of each of these minerals is determined by the contents of the interstack space: In

murmanite Na and P are replaced by water molecules, with the consequence that there is a shortening of the period *c* by 2.7 Å and a less strong binding between the stacks. As shown by the given investigation, in the transition from lomonosovite to murmanite marked changes occur also in the stack itself - both in its anion "networks" and in its cation "wall."

The middle part of the stack is a plane layer of close-packed (without gaps) octahedra of titanium and sodium. The Ti<sub>1-4</sub> octahedra, joined via edges, form brookite columns extending along the shortest period A (5.3 Å × 2). The titanium octahedra of the columns

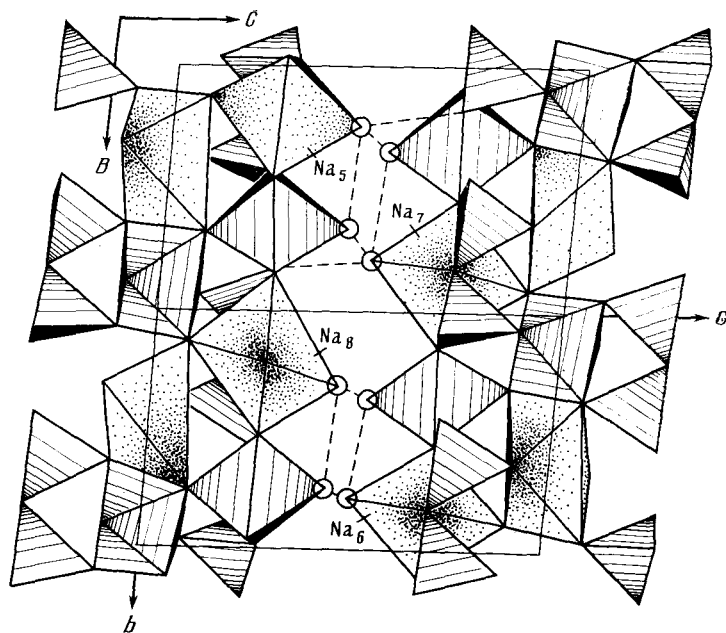


FIG. 2. Projection of structure on (100). Dotted shading marks polyhedra of sodium positions; circles are H<sub>2</sub>O molecules; dashed lines are hydrogen bonds.

are of the same dimensions (mean Ti-O range from 1.98 to 2.03 with edges 2.79-2.84 Å) and are scarcely suitable for accommodation of any of larger  $Mn^{2+}$  as done in Ref. 1. Moreover, according to the chemical analysis data,<sup>9,10</sup> the large cell has from 0.3 to 0.5 Mn atoms, and for this reason this element cannot pretend to an independent position. It is possible that together with Ti in the population of the columns  $Fe^{3+}$  statistically take part (0.3-0.6 atoms per cell). The shortest edges in the titanium octahedra are common:  $Ti_1$  contacts  $Ti_4$  and  $Ti_3$  along the edges  $O_2-O_{31} = 2.34$  and  $O_{13}-O_{18} = 2.66$  Å;  $Ti_2$  contacts  $Ti_3$  and  $Ti_4$  along the edges  $O_1-O_{20} = 2.43$  and  $O_{11}-O_{12} = 2.55$  Å. For the other edges 2.74-3.23, 2.58-3.19, 2.68-3.06, and 2.64-3.06 Å in the  $Ti_{1-4}$  octahedra, respectively.

Between the Ti columns spaced half a translation along B, there are Na columns made of polyhedra of two types. If in the  $Na_1$  and  $Na_4$  octahedra the Na-O distances range from 2.09 to 2.77 and from 2.07 to 2.85 Å, then in the second pair of octahedra the cations are strongly displaced toward one vertex and lose their bond with the other: The distances from  $Na_2$  and  $Na_3$  to the vertices of the hemioctahedra are 2.08-2.57 and 2.08-2.63 Å, while to the "departing" vertices they are 3.01 and 3.13 Å respectively. Thus in the construction of the murmanite sheets Na octahedra take part (as also in lomonosovite<sup>7</sup>) and Na pyramids similar to betalomonosovite.<sup>8</sup> Both the octahedral and the pyramidal positions of  $Na_{1-4}$  are filled statistically with a probability of 50%; the two positions  $Na_2$  and  $Na_3$  converge through 2.6 Å and cannot be simultaneously occupied. One of the variants of filling of the Na positions in the wall is shown in Fig. 1.

The layers against the two sides of the sheet (networks, chain-mail), in spite of Ref. 1, retain the architecture of lomonosovite (betalomonosovite): infinite bands of alternating Ti and Na polyhedra extending along B. The  $Ti_{5-8}$  octahedra in the chain mail are similar in size (mean Ti-O is 1.89-2.03 Å). Taking into consideration the increased weight of the  $Ti_7$  and  $Ti_8$  peaks on the electron density map, we can reckon that in these positions as well as Ti there are statistically distributed impurity atoms of Nb. For all the Ti atoms of the network there is characteristic marked anisotropy of the distances to the surrounding ligands, with maximum (or second longest) distances to the  $H_2O$  molecules.

The Na polyhedra of the network are differentiated in form and dimensions. The most compact is the  $Na_5$  octahedron with uniform distribution of the cation-anion distances: from 1.98 to 2.19 Å, mean 2.09 Å. Considering that the weight of the peak in this position on the electron density map is maximal, we can with a large degree of probability consider it to be statistically populated by heavy impurity cations  $Mn^{2+}$ ,  $Fe^{2+}$ , Zr, Nb, and to the least degree, Na.

On the other hand, the positions  $Na_6$  and  $Na_7$  form a loose octahedron (mean Na-O = 2.41 Å) and an eight-pointed figure (mean Na-O = 2.51 Å) with allowance for the weight of the peaks corresponding to the compositions  $Na_{0.4}Ca_{0.6}$  and  $Na_{0.8}K_{0.2}$ , respectively. The eight-pointed figure ( $Na_7$  bipyramid) has in common with the adjacent Ti octahedra of the network and the Si tetrahedra of both

diorthogroups edges of hexagonal section, and with the Ti octahedron sheets it is joined by the pyramid vertex; the second (free) vertex is occupied by an  $N_2O$  molecule. The octahedra  $Na_6$  and  $Na_7$  for the bond with the Ti octahedra of the network use two edges of the tetragonal cross section, and to the sheet they adjoin by a vertex; the opposites are also occupied by water molecules.

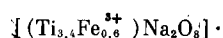
Finally, the fourth position of the network ( $Na_8$ ) is essentially of the sodium type both in the dimensions of the polyhedron (a very distorted octahedron with mean Na-O = 2.26 Å) and in weight of the electron density peak. This polyhedron is in contact with the Ti octahedra both of the sheet and the chain-mail only via vertices and has in common an edge with Si tetrahedra of one of the diorthogroups. The free vertex of the polyhedron is occupied by  $H_2O$ .

The diorthogroups  $Si_2O_7$  (four per complete cell) differ in the relative orientation of the tetrahedra. This is because with equal dimensions of the Ti octahedra of the sheet, on which the diorthogroups rest via their "tips," the Na polyhedra of the network are different in their dimensions, and the diorthogroups fit onto them.<sup>11</sup> The angles made by the terminal and bridging ligands  $O_t-O_b-O_t$  vary over considerable ranges: from 80 to 155°. The degree of distortion of the diorthogroups is also indicated by the large scatter in the Si-O distances, also related to the possible isomorphic substitutions of Al,  $Fe^{3+}$ , and Mg for Si (Ref. 12).

The three-layer stacks of murmanite are joined by hydrogen bonds of water molecules, which enter the coordination polyhedra of titanium and sodium positions of the network (in spite of Ref. 1, these  $H_2O$  molecules are not free). The average distance between  $H_2O$  molecules of adjacent layers is 2.8 Å, which indicates fairly strong bonds between them. Within the layers the hydrogen bonds are weaker.

Crystal-chemical analysis shows that with decomposition of lomonosovite with its conversion to murmanite there is preserved the most stable part of the structure - a framework of titanium and silicon-oxygen polyhedra. Processes of leaching occur both in the interstack space and in the Na sublattice of the network and sheet. The rigid structure of the sheet prevents replacement of Na by any impurity elements, and when Na is removed from the sheet, vacancies arise. On the other hand, the Na positions of the openwork chain mail act as a landing ground for the atoms of various elements which compensate for the deficit of sodium. The isomorphism over wide limits, especially in the Na sublattice of the network, is apparently the basic cause of the changes in unit-cell parameters and the reduction of the symmetry of the crystal (in comparison with lomonosovite).

The inadequate quality of the crystal and consequently of the experimental set of intensities did not permit us to obtain information on the distribution of small quantities of impurity cations among the crystallographic positions. However, crystal-chemical analysis gives a basis to regard the most probable formula of murmanite with allowance for the main isomorphic substitutions as follows:





where the square brackets distinguish the cationic and anionic parts of the structure.

The authors thank Yu. V. Nekrasov for help in obtaining the set of experimental data and V. I. Simonov for unflinching interest in the work and helpful discussion of the results.

<sup>1)</sup> Modification and extension of the RENTGEN\*75 system for the NORD-100 and SM-4 computers.

<sup>1</sup>A. D. Khalilov, Kh. S. Mamedov, E. S. Makarov, et al., Dokl. Akad. Nauk SSSR **161**, 1409 (1965).

<sup>2</sup>V. I. Andrianov, Z. Sh. Safina, and B. L. Tarnopol'skii, Rentgen-75: An Automated System of Programs for Determining Crystal Structures [in Russian], Otd. Inst. Khim. Fiz. Akad. Nauk SSSR, Chernogolovka (1975).

<sup>3</sup>L. V. Bukvetskaya, T. G. Shishova, V. I. Andrianov, and V. I. Simonov, Kristallografiya **22**, 494 (1977) [Sov. Phys. Crystallogr. **22**, 282 (1977)].

<sup>4</sup>Yu. A. Pyatenko, Kristallografiya **17**, 773 (1972) [Sov. Phys. Crystallogr. **17**, 677 (1973)].

<sup>5</sup>Z. Shakked, Acta Cryst. A. **39**, 278 (1983).

<sup>6</sup>N. V. Belov, Essays in Structural Mineralogy [in Russian], Nedra, Moscow (1976).

<sup>7</sup>R. K. Rastsvetaeva, V. I. Simonov, and N. V. Belov, Dokl. Akad. Nauk SSSR **197**, 81 (1971) [Sov. Phys. Dokl. **16**, 182 (1971)].

<sup>8</sup>R. K. Rastsvetaeva, M. I. Sirota, and N. V. Belov, Kristallografiya **20**, 259 (1975) [Sov. Phys. Crystallogr. **20**, 158 (1975)].

<sup>9</sup>E. I. Semenov, N. I. Organova, and M. V. Kukharchik, Kristallografiya **6**, 925 (1961) [Sov. Phys. Crystallogr. **6**, 746 (1962)].

<sup>10</sup>N. I. Zabavnikova, in: Methods of Chemical Analysis of Minerals and Chemical Composition [in Russian], Nauka, Moscow (1967), p. 69.

<sup>11</sup>N. V. Belov, Crystal Chemistry of Silicates with Large Cations [in Russian], Izd. Akad. Nauk SSSR, Moscow (1961), 68 pp.

<sup>12</sup>Yu. A. Pyatenko, A. A. Voronkov, and Z. V. Pudovkina, Mineralogical Crystal Chemistry of Titanium [in Russian], Nauka, Moscow (1976).

Translated by S. G. Kirsch

## Nonisostructural compounds of copper (I) chloride and bromide with allyl cyanide: synthesis and crystal structure of $\pi$ complexes $2CuX \cdot CH_2=CHCH_2CN$ ( $X=Cl, Br$ )

P. Yu. Zavali, M. G. Mys'kiv, and E. I. Gladyshevskii

State University, L'vov

(Submitted September 28, 1984)

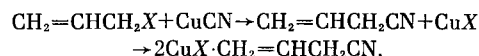
Kristallografiya **31**, 88-92 (January-February 1986)

The authors make an x-ray structural analysis of complexes of CuCl and CuBr with allylcyanide. The complexes are nonisostructural, but are of similar structure: the inorganic part (CuX) of the structure consists of layers formed by "stepped" tetramers  $Cu_4X_4$  and joined by bridging ligands into a framework. The difference between these structures appears in the positions of the molecules of allyl cyanide, in which the torsion angles  $C=C-C$  differ markedly.

The structure of the cyanoolefin complexes of copper (I) are of interest both for interpretation of the mechanism of Meierwein's reaction<sup>1</sup> and also from the viewpoint of the influence of the cyano group on the coordination capacity of the C=C bond. At present structural studies have been made on compounds of CuX with olefins containing only a cyano group conjugate with the C=C bond (acrylonitrile,<sup>2</sup> methylacrylonitrile,<sup>3</sup> crotononitrile,<sup>4</sup> and fumaronitrile<sup>5</sup>). Of these only the first is a  $\pi$  complex.

Continuing our work on the structure of complexes of copper (I) halides with substituted olefins (allyl alcohol,<sup>6</sup> acrylic acid,<sup>7</sup> acrylamide, fumarodinitrile,<sup>5</sup> and maleic acid<sup>8</sup>) we made an x-ray structural investigation of the new complexes  $CuX$  ( $X=Cl, Br$ ) with allylcyanide ( $AllCN$ ).

The investigated compounds  $2CuX \cdot AllCN$  were obtained in the process of synthesis of allylcyanide from the corresponding allylhalide and CuCN:



When  $AllCl$  and CuCN are boiled together for 30 h there are formed crystals of complex I, suitable for x-ray structural analysis, whereas compound II is formed in an

hour in the form of a finely crystalline deposit. Larger crystals are obtained by keeping the saturated solution of CuBr in  $AllCN$  at 273 K.

The colorless crystals of  $2CuX \cdot AllCN$ , stable in air in the absence of moisture, were investigated by the photographic method and in a Syntex automatic diffractometer with Mo  $K\alpha$  radiation and a graphite monochromator (Table I). The integral intensities were corrected for the Lorentz and polarization factors. No correction was made

TABLE I. Crystallographic Data on Structures of  $2CuX \cdot AllCN$

Characteristics	I	II
Composition	$2CuCl \cdot C_3H_5N$	$2CuBr \cdot C_3H_5N$
<i>a</i> , Å	8.358(3)	7.596(3)
<i>b</i> , Å	7.457(2)	7.330(3)
<i>c</i> , Å	11.851(3)	14.259(5)
$\gamma$ , deg	98.77(3)	97.59(3)
<i>V</i> , Å <sup>3</sup>	730.0(4)	786.3(6)
$\mu$ , cm <sup>-1</sup>	66.6	162.6
<i>F</i> (000)	512	656
$\rho_{calc}$ , g/cm <sup>3</sup>	2.41	2.99
<i>Z</i>	4	4
Space group	$P2_1/b$	$P2_1/b$
Diffractometer	<i>P1</i>	<i>P2</i>
Scanning	$\theta/2\theta$	$\omega$
$2\theta$ , deg	48	50
No. of reflections	530	1051
<i>R</i>	0.053	0.060